Talanta 82 (2010) 803–809

Contents lists available at ScienceDirect

Talanta

journal homepage: www.elsevier.com/locate/talanta

Label-free optical diagnosis of hepatitis B virus with genetically engineered fusion proteins

Shun Zheng[a], Do-Kyun Kim[b], Tae Jung Park[b,*], Seok Jae Lee[c], Sang Yup Lee[a,b,d,**]

[a] Department of Chemical & Biomolecular Engineering (BK21 program), KAIST, 335 Gwahangno, Yuseong-gu, Daejeon 305-701, Republic of Korea
[b] BioProcess Engineering Research Center, Center for Systems & Synthetic Biotechnology, and Institute for the BioCentury, KAIST, 335 Gwahangno, Yuseong-gu, Daejeon 305-701, Republic of Korea
[c] NEMS-Bio Team, National Nanofab Center, 335 Gwahangno, Yuseong-gu, Daejeon 305-806, Republic of Korea
[d] Department of Bio & Brain Engineering, Department of Biological Sciences, and Bioinformatics Research Center, KAIST, 335 Gwahangno, Yuseong-gu, Daejeon 305-701, Republic of Korea

ARTICLE INFO

Article history:
Received 3 April 2010
Received in revised form 26 May 2010
Accepted 27 May 2010
Available online 4 June 2010

Keywords:
Surface plasmon resonance
Localized surface plasmon resonance
Biosensor
Hepatitis B virus
Gold-binding polypeptide
Fusion protein

ABSTRACT

A simple biosensing strategy for the diagnosis of patients with hepatitis B virus (HBV) was developed. This study can be divided into two themes, both of which utilized gold-binding polypeptide (GBP) fusion proteins: HBV surface antigen PreS2 (HBsAg) detection with GBP-fused single chain antibody (GBP-ScFv) and anti-HBsAg detection with GBP-HBsAg. These GBP-fusion proteins can directly bind onto the gold surface *via* the high binding affinity between the GBP and the gold surface, while at the same time, orient the recognition sites toward the sample for target binding. This one-step immobilization strategy, which greatly simplifies a fabrication process as well as maintaining biological activity of the recognition elements, can be applied to optical analytical methods, such as surface plasmon resonance (SPR) and localized surface plasmon resonance (LSPR).

1. Introduction

Biosensors have increasingly become practical and useful tools in the development of equipment used in medicine and food quality control, environmental monitoring and research [1]. The immobilization of biological elements, typically proteins such as enzymes and antibodies, is a key step for the construction of a biosensing system. Various methods have been described for this purpose. One method involves the adsorption on insoluble matrices *via* van der Waals forces, ionic binding or hydrophobic forces. This is a simple process which causes little disruption to the proteins while it is unstable during the binding process because of the highly dependency on environmental condition, such as pH, solvent and temperature, in maintaining its functional characteristics. Another method involves the entrapment of biological elements in a gel, forming a semipermeable membrane on a solid surface. This is a universal platform suitable for any proteins. However, the construction of this system results in diffusional barriers, loss of sensing element by leakage and possible denaturation of the proteins as a result of free radicals. Biosensing systems can also be constructed by cross-linking multifunctional reagents by a certain number of functional groups, such as glutaraldehyde bis-isocyanate derivatives or bis-diazobenzidine, due to its simple and strong chemical binding procedure of proteins. This is widely used for the stabilization of physically adsorbed proteins that are covalently bound onto a support platform. However, this method also has disadvantages, for example, the difficulty in controlling the cross-linking reaction, the gelatinous nature and the relatively low activity of the proteins due to the specific structural features. The last method commonly used is the covalent binding of protein onto insoluble supports, forming a stable enzyme-support complex where leakage of the biomolecule is very unlikely and thus, is ideal for mass production and commercialization. However, this method is complex, time-consuming, and can possibly lead to activity losses of the proteins due to the protein-modification reactions involving essential groups for the biological activity [2]. In each of these methods used for the construction of a biosensor-exhibiting favorable performance, a number of factors deserve careful consideration, such as strong binding forces between the solid surface and recognition elements, exposure of active sites to sample solu-

* Corresponding author. Tel.: +82 42 350 8814; fax: +82 42 350 8800.
** Corresponding author at: BioProcess Engineering Research Center, Center for Systems & Synthetic Biotechnology, and Institute for the BioCentury, KAIST, 335 Gwahangno, Yuseong-gu, Daejeon 305-701, Republic of Korea.
Tel.: +82 42 350 3930; fax: +82 42 350 8800.
E-mail addresses: tjpark@kaist.ac.kr (T.J. Park), leesy@kaist.ac.kr (S.Y. Lee).

0039-9140/$ – see front matter © 2010 Elsevier B.V. All rights reserved.
doi:10.1016/j.talanta.2010.05.059

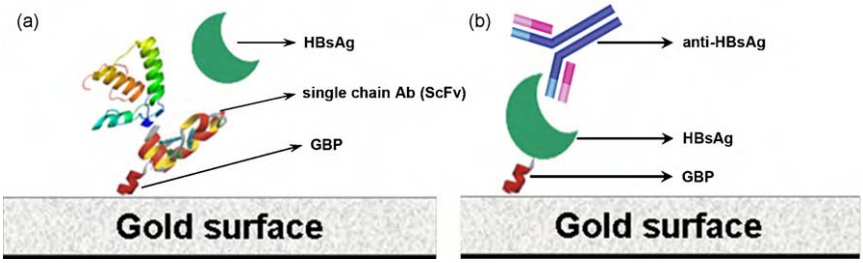

Fig. 1. Schematic diagram of bio-recognition element onto the gold surface by GBP-fusion proteins. (a) Immobilization of single chain variable fragment antibody *via* 6HGBP-ScFv fusion protein for the detection of HBsAg; (b) HBsAg immobilization *via* GBP-HBsAg protein for the detection of anti-HBsAg.

tion, conservation of bioactivity after immobilization, and easy handling.

Recently, many polypeptide sequences, which can specifically bind to metals (Au, Ag, Pt) [3–5], oxides (ZnO, Cu_2O, $CaCO_3$) [6,7], and semiconductors (CdS, ZnS) [8,9], have been selected using *in vivo* combinatorial biotechnology, e.g., either phage or cell surface display techniques. Among them, gold-binding polypeptide (GBP) with a specific amino acid sequence (H_2N-MHGKTQATSGTIQS-COOH) is one of the examples of genetically engineered peptides for inorganics [3]. The strong binding property of GBP was found to be due to the presence of a three repeat of this amino acid sequence (GBP3) [10,11]. Interestingly, whereas many proteins and self-assembled monolayers bind to the gold surface *via* thiol linkage, GBP does not contain a cysteine residue, which is known to form a covalent bond with the gold surface *via* thiol group. Although the definite mechanism is not clear yet, it is estimated that, since GBPs are rich in serine and threonine, these polar groups seem to coordinately interact with the gold surface, forming a monolayer observed by atomic force microscopy [12,13]. In addition, Tamerler et al. applied a quartz crystal microbalance technique (QCM) and surface plasmon resonance (SPR) to investigate the kinetics and thermodynamics of biomimetic interactions between the GBP and the gold surface [14,15]. They also demonstrated that the GBP binds fairly tightly to the gold surface due to the lower standard Gibbs free energy (comparable to other thiol-based systems) of the bond, and the binding process is fast under aqueous conditions compatible with biological environments [13–15]. These characteristics suggest its potential application in nano- and bio-technologies as novel agents for surface functionalization.

In view of these previous works, we here employed GBP-fusion proteins in the construction of SPR-based biosensors for the hepatitis B virus (HBV) diagnosis *via* the dual-detection of HBV surface antigen PreS2 (HBsAg) and anti-HBsAg antibody (anti-HBsAg) (Fig. 1). The strong affinity between the GBP and the gold surface guarantees the stability of this sensor system and orients the sensing parts outward from the solid surface, exposing them directly to the sample solution. This platform, by mediating the recognition parts and the solid surface with GBP, alleviates the problem of activity loss, owing to lack of frigidity, when the parts are immobilized on the solid surface. Since the gold has been a very versatile material in the field of biosensors, two different kinds of detecting basis were developed to validate these systems, which are optical signal-based detections including SPR and localized surface plasmon resonance (LSPR) [13,14,16]. All of them obviate the labeling step and can directly detect targets in sample solution.

2. Experimental

2.1. Chemicals and reagents

Restriction enzymes and DNA modifying enzymes were purchased from New England Biolabs (Berverly, MA, USA). Agarose was from Cambrex BioScience Rockland (Rockland, ME, USA). 30% (w/v) acrylamide/bis solution and protein assay were purchased from Bio-Rad (Hercules, CA, USA). HBsAg PreS2 peptide (H_2N-NSTTFHQALLDPRVRGLYFPAGG-COOH) and its specific rabbit-immunized polyclonal anti-HBsAg antibody were synthesized at Peptron (Daejeon, Korea). Ni-NTA spin kit was from Qiagen (Hilden, Germany). Other chemicals and reagents were purchased from Sigma (St. Louis, MO, USA), unless otherwise stated. All oligonucleotides were synthesized at Genotech (Daejeon, Korea).

2.2. Apparatus

Polymerase chain reaction (PCR) experiments were performed with a PCR Thermal Cycler (Bio-Rad, Hercules, CA, USA) using High Fidelity PCR System (Boehringer Mannheim, Mannheim, Germany). DNA sequences were confirmed by automatic DNA sequencer (ABI Prism model 377, Perkin Elmer Co., Grove, IL, USA). Cell growth was monitored by measuring the absorbance at 600 nm (OD_{600}; DU®650 Spectrophotometer, Beckman, Fullerton, CA, USA). Cells were disrupted by sonication (Braun Ultrasonics Co., Danbury, CT, USA). SPR analysis was performed with BIAcore3000™ (Biacore, Uppsala, Sweden). The various metal depositions were achieved by E-beam evaporator (MHS 1800, MooHan Co. Ltd., Korea) and LSPR signal was obtained with an LSPR spectroscopy system (Ocean Optics Inc., Dunedin, USA).

2.3. Production of GBP-fusion proteins

The flowchart of fusion protein construction is shown in Fig. S1 (see Supplementary Information). The 6HGBP-ScFv fusion protein was prepared by genetically fusing the GBP and ScFv, allowing two specific interactions between GBP and gold substrates, and the capture of HBsAg and anti-HBsAg, respectively. For easy purification of the fusion protein by metal affinity chromatography, the coding sequence of a six-histidine (6H) was introduced at the N-terminus of the GBP. For the cloning of the fusion gene, the DNA fragments encoding 6HGBP (six-histidine fused GBP) were obtained by PCR amplification using plasmid pTacFadLGBP-3 [17] as a template, and P1 (5′-AAAATACCATATGGGCCACCATCACCATCACCACGG-3′) and P2 (5′-TTCCCCATGGAGACGAATGGTACCGCTCGT-3′) as primers. The PCR product was digested with NdeI and NcoI, and ligated into the same sites of pET-22b(+) (Novagen, San Diego, CA, USA) to make pET-6HGBP. For the cloning and expression of the 6HGBP-ScFv fusion gene, the DNA sequence encoding anti-HBsAg fragment was amplified by PCR using plasmid pET-ScFv-SBD [18] as a template, and P3 (5′-CAAGACCATGGGTGTCGACTGAGGAGTCTGGA-3′) and P4 (5′-TCCGCTCGAGACGTTTTATTTCCAGGTAGGT-3′) as primers. This PCR product was digested with NcoI and XhoI, and ligated into the same sites of pET-6HGBP to make pET-6HGBP-ScFv.

Escherichia coli BL21(DE3) [F^- *ompT hsdS*$_B$ ($r_B^-m_B^-$) *gal dcm* (DE3)] was used as a host strain for the expression of GBP-fused anti-HBsAg fragment (GBP-ScFv). Recombinant *E. coli* BL21(DE3) strain harboring pET-6HGBP-ScFv was cultivated in 250 mL flasks

containing 100 mL Luria–Bertani medium supplemented with 2% (w/v) glucose and 100 μg mL^{-1} of ampicillin at 37 °C in a rotary shaking incubator. Cell growth was monitored by measuring the absorbance at 600 nm. At an OD_{600} of 0.4, isopropyl-β-D-thiogalactopyranoside (IPTG) was added to a final concentration of 1 mM to induce protein expression. Then, cells were further cultivated for 6 h and harvested by centrifugation. Cells were disrupted by sonication for 1 min at 40% output and centrifuged at 16,000 × *g* for 10 min at 4 °C. The pellet containing insoluble proteins was denatured, purified and underwent dialysis for further experiments. Since the 6HGBP-ScFv fusion protein contains six-histidine tag at N-terminal, they could be simply purified using Ni-chelating resin (Qiagen, Valencia, CA, USA) without further purification step. Protein concentration was determined by standard Bradford's method using bovine serum albumin (BSA) as a standard. Upon calculation, the size of 6HGBP-ScFv fusion protein is about 60.4 kDa. According to the result, purified 6HGBP-ScFv fusion protein was with good purity and quantity for further use. The GBP-HBsAg fusion protein was synthesized and characterized by high-performance liquid chromatography (HPLC) and MALDI-TOF (see Fig. S2) analysis according to the manufacturer's procedure (Peptron).

2.4. SPR spectroscopy analysis for HBV diagnosis

For HBsAg detection, the concentration of 6HGBP-ScFv fusion protein was roughly optimized at first. Sequential injection of solutions was as follows: for equilibration, phosphate-buffered saline (PBS) solution was flowed over the bare gold surface to wash away any potential contaminants. Then, several different concentrations of 6HGBP-ScFv fusion protein were injected. The optimal concentration of 6HGBP-ScFv fusion protein, determined in this process, was used for detecting various concentrations of target HBsAg in the following experiments. In the process of HBsAg detection, BSA instead of the target was injected as a negative control. Prior to the target binding, 0.5 mg mL^{-1} of BSA was injected for an effective blocking of any nonspecific binding sites. In order to remove non-specifically bound molecules and unbound targets, washing step was applied intermittently with PBS for about 5 min. For the binding of targets, a fixed flow rate at 20 μL min^{-1} and binding time of 5 min was applied, consuming a total sample volume of 100 μL.

SPR detection of anti-HBsAg antibody was similar to the experimental procedure described above, while BSA was used as a blocking reagent and a negative control, and anti-mouse immunoglobulin G (IgG) in case of antibody detection were used as a negative control.

2.5. Fabrication of multi-spot LSPR chip and set up of optical spectroscopy system for HBV diagnosis

To fabricate multi-sport gold-capped nanoparticle array (MG-NPA) chip, the surface-modified silica nanoparticles (100 nm in diameter) were aligned onto the gold-deposited glass substrate. For the surface modification of silica nanoparticles, they were mixed with 1% (v/v) 3-aminopropyltriethoxy silane (γ-APTES) solution in ethanol by continual stirring at room temperature for 24 h. The modified silica nanoparticles were then prepared at 1% (w/v) by dispersing in ultrapure deionized (DI) water. After cleaning of the glass substrate, the Cr layer (5 nm) and the bottom Au layer (40 nm) were deposited onto the glass substrate with the E-beam evaporator at a base pressure of 4×10^{-6} Torr. For the fabrication of multi-spot type chip, a 15-spot (5 mm in diameter) silicon-rubber mask was carefully placed on the surface of Au-deposited slide glass. Then, 1 mM 4,4′-dithiodibutyric acid (DDA) was introduced to the Au-layered surface and left for 1 h at room temperature to allow the formation of a self-assembled monolayer (SAM) of the DDA. Surface-activated silica nanoparticles and 400 mM 1-ethyl-3-(3-dimethylaminopropyl) carbodiimide (EDC) were then mixed 1:1 and introduced to the activated SAM formation for 1 h. Finally, a top Au layer (30 nm) was deposited onto the nanoparticle layer using the E-beam evaporator. This kind of MG-NPA chips was in agreement with the well-known properties that provided a suitable platform for an LSPR-based analysis as previous reports [16,19].

After these fabrication procedures, the optical characteristics of the MG-NPA chip surface were evaluated in the absorbance spectra range of 450–750 nm using the LSPR spectroscopy system at room temperature. The LSPR spectroscopy system consists of a tungsten halogen light source (LS-1, wavelength range 360–2000 nm), spectrophotometer (USB2000 UV-visible, wavelength range 250–1100 nm), an optical probe bundle (R-400-7 UV-visible, fiber core diameter 200 μm, wavelength range 250–850 nm) and computer. In this optical detection system, the arrangement of the optical probe is a tight bundle of seven fibers, six illumination fibers around one detector fiber. The outer six illumination fibers connect to the light source and the detector fiber couples to a spectrophotometer. The absorbance data were analyzed using Spectra Suite software (Ocean Optics Inc., Dunedin, USA).

For the detection of HBsAg and anti-HBsAg antibody, 6HGBP-ScFv and GBP-HBsAg fusion proteins were immobilized on each MG-NPA chip surface by incubating for 1 h at room temperature, respectively. Then, different concentrations (1 fg mL^{-1} to 10 μg mL^{-1}) of each target reagent were incubated on the MG-NPA chip surface for 1 h, thoroughly washed with DI water and dried with nitrogen gas. Then, an LSPR spectroscopy system was used for LSPR signal acquisition and data evaluation. Upon sequential introducing the fusion proteins and its target proteins, there are changes in the refractive index (RI) of the MG-NPA chip surface and this reflected in an increase in absorbance, enabling detections of the biomolecular species of interest [20].

3. Results and discussion

3.1. Preparation of 6HGBP-ScFv fusion protein

For expression of the fusion proteins, *E. coli* BL21(DE3) was used as a host strain. Fig. S3 shows the sodium dodecyl sulfate polyacrylamide gel electrophoresis (SDS-PAGE) profile of 6HGBP-ScFv fusion protein expression with a purification result. Compared with the wild type *E. coli* BL21(DE3) strain as a negative control, *E. coli* BL21(DE3) harboring pET-6HGBP-ScFv expresses a thick band between marker bands of 27.5 and 37 kDa. This band size is in agreement with the size of protein 6HGBP-ScFv, which was calculated as approximately 31.9 kDa. Since this fusion protein is expressed as an insoluble fraction, it was purified in denaturing condition and sequentially subjected to dialysis. The most right band shows the purified fusion protein through Ni-chelating column resulting with good purity and quantity for further use in several sensing platforms.

3.2. HBV diagnosis by SPR analysis

Detection of HBV was performed using commercial SPR to confirm the successful binding of a series of molecules. To investigate the detection of HBV surface antigen, 6HGBP-ScFv concentration was first optimized as follows: 100, 50 and 10 μg mL^{-1} of 6HGBP-ScFv fusion protein was flowed over the gold surface, respectively. The fusion protein 6HGBP-ScFv was immobilized onto the gold surface *via* its intrinsic affinity with the gold as shown in Fig. 2. Interestingly, coverage of 6HGBP-ScFv on the gold surface did not always increase with increasing protein concentration,

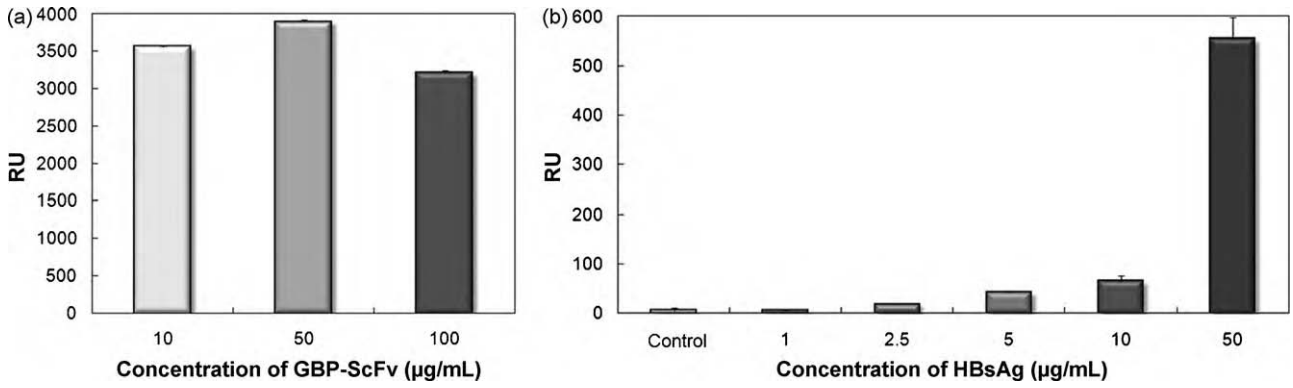

Fig. 2. Molecular binding optimization of GBP-ScFv fusion protein and its target antigen, HBsAg, with different concentrations by using SPR experiments. (a) Binding affinities with different concentrations of 6HGBP-ScFv fusion protein. (b) Statistical detection profiles of target antigen with 6HGBP-ScFv of 50 μg mL^{-1} as a receptor. BSA of 50 μg mL^{-1} was used as a negative control.

a maximal resonance unit (RU) change appearing at concentration of 50 μg mL^{-1}. From this result, 6HGBP-ScFv concentration of 50 μg mL^{-1} was chosen for following experiments.

Next, we checked the specificity of this platform with BSA as a negative control. Fifty μg mL^{-1} of 6HGBP-ScFv was injected into the fluid phase, followed by 0.5 mg mL^{-1} BSA blocking to reduce nonspecific binding. In order to investigate the selectivity and sensitivity of target analyte, 50 μg mL^{-1} of BSA as a negative control to compare with target HBsAg, different concentrations (1, 2.5, 5, 10 and 50 μg mL^{-1}) of target HBsAg were injected into respective channels, respectively. Below concentrations of 50 μg mL^{-1} for HBsAg, RU levels dropped rapidly while target concentrations as low as 2.5 μg mL^{-1} can be detected compared with the control. For 1, 2.5, 5, 10 and 50 μg mL^{-1} of target HBsAg, and 50 μg mL^{-1} of BSA, RU increase is 4.9, 17.4, 48.5, 55.7, 542.2 and 5.6 RU, respectively, showing an increasing trend of SPR signals with increasing concentration of target within this scope. In the BIAcore SPR system, 1000 RU corresponds to a 0.01° change in SPR angle, a 1.0 ng mm^{-2} change in surface mass, and a bulk refractive index change of 0.001 [21]. In view of molecular weight of HBsAg, and chip surface area where covered by microfluidic channels, the binding of 2.5 μg mL^{-1} HBsAg represents the binding of about 8.3×10^{12} molecules to the gold surface.

Since the successful detection of HBV antigen, specific detection experiment for HBV antibody was also performed. For the detection of anti-HBsAg, GBP-HBsAg fusion protein was first immobilized onto the gold surface. The concentrations of the GBP-HBsAg fusion protein were optimized as follows by flowing over the gold surface to 250 μg mL^{-1}, 500 μg mL^{-1}, 1 mg mL^{-1} and 2 mg mL^{-1}, respectively. These fusion protein molecules were immobilized onto the gold surface *via* its intrinsic affinity with the gold. GBP-HBsAg was dissolved in water because it tended to aggregate in PBS solution and resulted in a decrease in RU value during its binding to the gold surface. As shown in Fig. 3a, GBP-HBsAg coverage on the gold surface increased with increasing concentration and a maximal RU change appearing at the concentration of 1 mg mL^{-1} GBP-HBsAg. Thus, the concentration of 1 mg mL^{-1} GBP-HBsAg was chosen for further experiments. When the concentrations of 6HGBP-ScFv and GBP-HBsAg were higher than 50 μg mL^{-1} (Fig. 2a) and 1 mg mL^{-1} (Fig. 3a), respectively, the resonance units decreased. Some of the binding sites may have been compromised, because the GBP-fusion proteins were densely immobilized on the gold surface and thus steric hindrance between closely neighbored GBP-fusion molecules may have occurred. Therefore, these results indicate that the best packing density of GBP-fusion proteins was obtained using the solution concentrations of 50 μg mL^{-1} (Fig. 2a) and 1 mg mL^{-1} (Fig. 3a), respectively. This particular packing density of the GBP-fusion proteins likely reduced steric hindrance, provided sufficient binding sites to the gold surface for biosensing their targets, and avoided loss of biological activity.

Then, the detection specificity of this platform was checked using anti-mouse IgG as a negative control. First, 1 mg mL^{-1} of GBP-HBsAg was injected followed by 0.5 mg mL^{-1} BSA blocking, then, 10 μg mL^{-1} anti-mouse IgG as a negative control, 1, 5 and 10 μg mL^{-1} of target anti-HBsAg was injected to respective channels. In each case, RU value increase is 5.9, 75, 278 and 278 RU, respectively, showing that limit of detection (LOD) lay between 1 and 5 μg mL^{-1} of target (Fig. 3b). SPR signal increase is increasing with target concentration of anti-HBsAg.

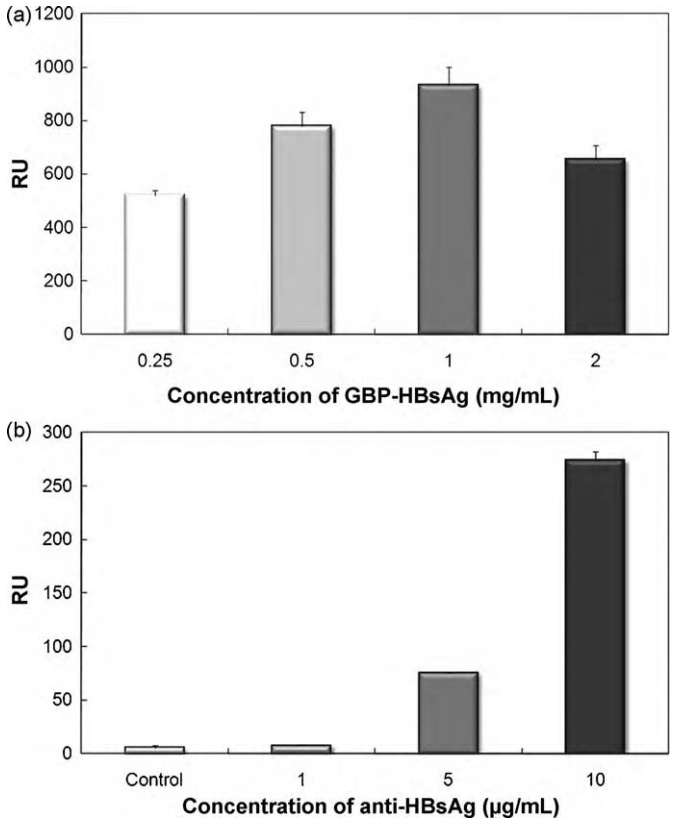

Fig. 3. Molecular binding optimization of GBP-HBsAg fusion protein and its target antibody, anti-HBsAg, with different concentrations by using SPR experiments. (a) Binding affinities with different concentrations of GBP-HBsAg fusion protein. (b) Statistical detection profiles of target antibody with GBP-HBsAg of 1 mg mL^{-1} as a receptor. Anti-mouse IgG of 10 μg mL^{-1} was used as a negative control.

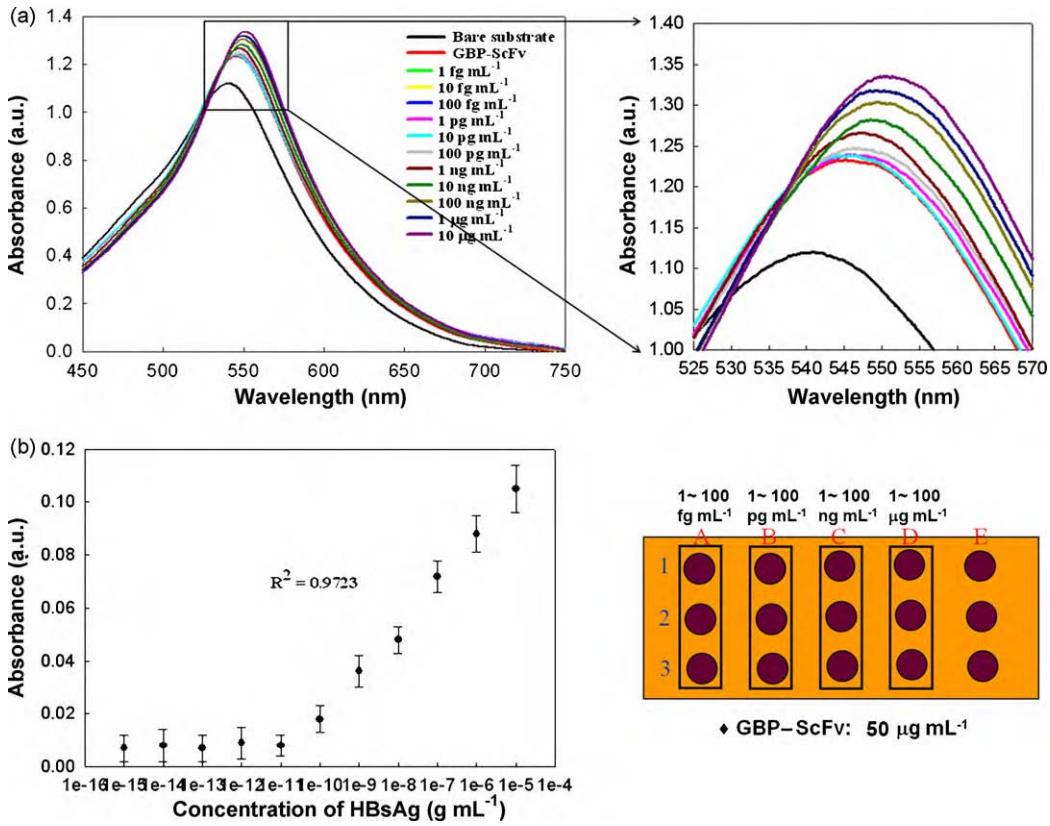

Fig. 4. Optical characteristics obtained after interaction of 50 μg mL^{-1} 6HGBP-ScFv with serial dilutions of HBsAg. (a) Superimposed spectroscopy profiles obtained in presence of HBsAg with various concentrations. (b) Quantitative calibration curve for absorbance dependence on HBsAg concentration from 1 fg mL^{-1} to 10 μg mL^{-1} by using 6HGBP-ScFv immobilized on the 15 MG-NPA chip.

It is worthy of mention that the LOD of anti-HBsAg antibody is higher than that of HBsAg according to SPR experiments. This seems odd since a size and a molecular weight of anti-HBsAg is much larger than HBsAg, which should lead to an easier detection or lower LOD. As proteins are a set of extremely sensitive molecules, which are only active when they can maintain their natural 3D configuration, fusion with other molecules will inevitably affect their activities. Because of the smaller size of HBsAg compared to anti-HBsAg, it seems that GBP-fusion proteins affected the active sites of HBsAg more seriously than anti-HBsAg. Another explanation of the differences in LOD might be the high density of the immobilized GBP-HBsAg. Since a size of GBP-HBsAg is smaller than that of GBP-ScFv, packing density and steric hindrance exhibited a severe impact on anti-HBsAg detection.

3.3. *HBV diagnosis by LSPR spectroscopy system with MG-NPA chip*

Since a successful detection of HBV with SPR, LSPR experiments were subsequently carried out to explore a detection signal enhancing. Differing from SPR, in the case of metal nanostructures, plasmon oscillations are localized and not characterized by propagation constant as in the case of SPR [22]. The collective charge density oscillations of the nanostructures are defined as LSPR [16,19]. Theoretically, the LSPR is excited when the electromagnetic radiation of incident light interacts with the free electrons of the nanostructures, which results in the collective oscillations, leading to strong enhancements of the local electromagnetic fields surrounding the nanostructures [23,24]. The corresponding change in the absorbance intensity is an important detection signal for analytical and biological applications since the molecular interfaces are highly functionalized by biochemical reactions.

The absorbance intensity increments in the LSPR spectroscopy system were observed when various HBsAg concentrations of 1 fg mL^{-1} to 10 μg mL^{-1} were independently introduced onto the each spot on the MG-NPA chip. Every spots for the different concentrations were repeated three times. With the higher concentrations of HBsAg, the absorbance intensities of the LSPR spectra increased at a constant rate, denoting the interactions of HBsAg with 6HGBP-ScFv fusion proteins (Fig. 4a). The LSPR measurement appears to be highly sensitive for the detection of HBsAg concentrations at low levels. Even at 100 pg mL^{-1} of HBsAg, a distinct response in the absorbance intensity increase could be obtained (Fig. 4b). The dynamic range fell in the concentration range of 100 pg mL^{-1} to 10 μg mL^{-1}, showing a linear trend with increasing HBsAg concentration and an R^2 value of 0.9723 for Δ absorbance. Similarly, anti-HBsAg antibody detection was also performed with LSPR analysis. Operational procedure was all the same with HBsAg detection except for the use of different receptor reagents. The absorbance intensity change was recorded depending on the concentration of anti-HBsAg antibody as shown in Fig. 5a. The LOD was determined as 1 pg mL^{-1} of anti-HBsAg antibody with a wide dynamic linear range of 1 pg mL^{-1} to 10 μg mL^{-1} and R^2 value of 0.9772 for Δ absorbance (Fig. 5b). The optical characteristics of the LSPR-based biosensor using noble metal nanoparticles or metal nanoislands were commonly detected with the help of a shift in the peak wavelength. However, in the case of our MG-NPA chip with core–shell type nanostructure, we could observe a significant increase in the absorbance intensity using the chip constructed for the LSPR-based biosensor. These results suggested that a strong enhancement of the local electromagnetic field surrounding the core–shell type nanostructure due to the interaction with refractive index in the biomaterial layer part. Similarly, the increase in the absorbance intensity

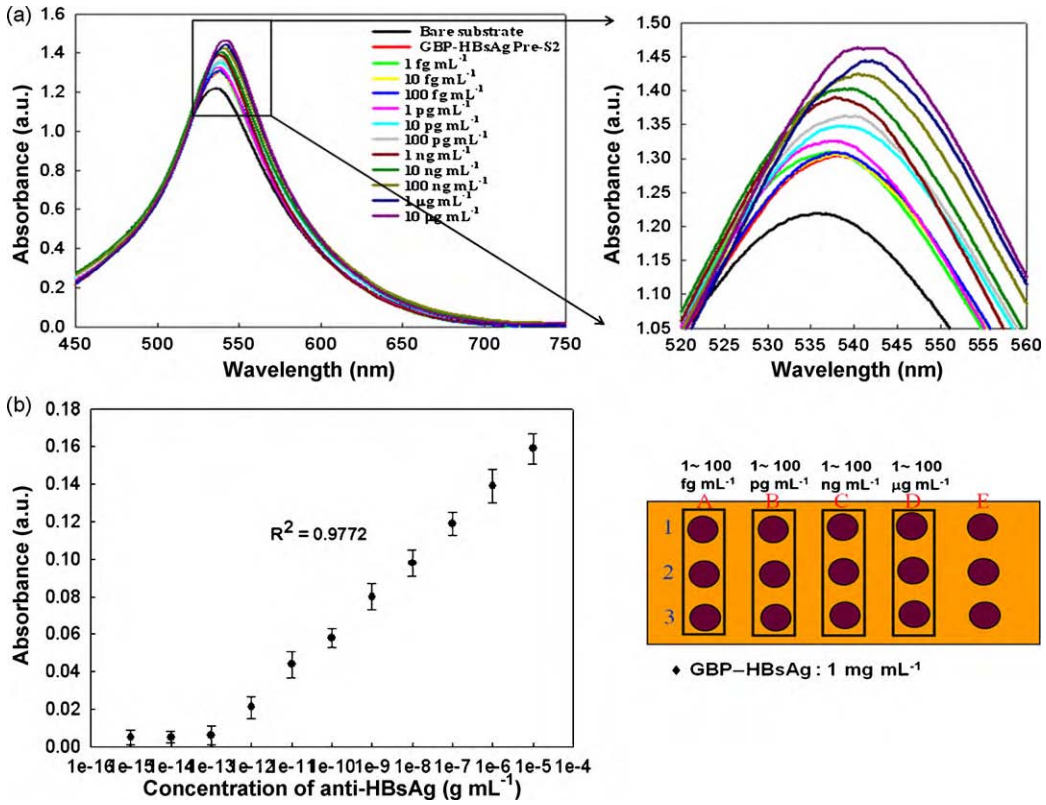

Fig. 5. Optical characteristics obtained after interaction of 1 mg mL^{-1} GBP-HBsAg with serial dilutions of anti-HBsAg antibody. (a) Superimposed spectroscopy profiles obtained in presence of anti-HBsAg antibody with various concentrations. (b) Quantitative calibration curve for absorbance dependence on anti-HBsAg antibody concentration from 1 fg mL^{-1} to 10 μg mL^{-1} by using GBP-HBsAg immobilized on the 15 MG-NPA chip.

along with the increasing layer thickness was reported previously [18,25–27].

This LSPR method has developed the major share of the attention in biosensor applications for their various advantages such as high sensitivity and specificity, permits them to rival the most advanced optical protocols. For the determination of optimal 6HGBP-ScFv and 6HGBP-HBsAg coverage, its concentrations, time and other conditions for molecular bindings were carefully calculated in regard to that used in SPR analysis.

4. Conclusion

In conclusion, several methods for HBV diagnosis with GBP-fusion proteins were developed. First, 6HGBP-ScFv was prepared from simple cultivation of recombinant *E. coli* for HBsAg detection and GBP-HBsAg was chemically synthesized for anti-HBsAg detection. These fusion proteins allowed for the direct and easy immobilization onto the gold surface. Successful binding of the proteins was demonstrated by various analytical methods due to versatile use of the gold substrate in the sensing area, such as SPR and LSPR analysis based on an optical detection mechanism. This process is very simple, requiring merely one step to immobilize the recognition element onto the solid surface; strong affinity between the GBP and the gold surface guarantees stability preventing possible leakage of sensing proteins; binding of GBP onto the gold surface also might help to expose sensing molecules outward to react with their targets; additionally, GBP prevents direct contact between proteins and the gold surface, which is advantageous for protein activity conservation. Both SPR and LSPR successfully present the effectiveness of this sensing platform. Especially, LSPR spectroscopy was carried out up to the concentration of attomolar level of target proteins. Regarding intrinsic advantageous property such as high sensitivity, the proposed method presented in this study has a huge potential in commercialization for HBV diagnosis. Furthermore, it is easy to conclude that a device capable of detecting multiple targets can be designed since the bio-recognition elements against targets (e.g. antibody or aptamer) can be easily fused with GBP *via* recombinant DNA technology or linker chemistry.

Acknowledgements

This work was supported in part by the IT Leading R&D Support Project from the MKE through KEIT and by WCU (World Class University) program through the National Research Foundation of Korea funded by the Ministry of Education, Science and Technology (R32-2008-000-10142-0).

Appendix A. Supplementary data

Supplementary data associated with this article can be found, in the online version, at doi:10.1016/j.talanta.2010.05.059.

References

[1] J. Castillo, S. Gaspar, S. Leth, M. Niculescu, A. Mortari, I. Bontidean, V. Soukharev, S.A. Dorneanu, A.D. Ryabov, E. Csoregi, Sens. Actuators B: Chem. 102 (2004) 179.
[2] W.H. Scouten, J.H.T. Luong, R.S. Brown, Trends Biotechnol. 13 (1995) 178.
[3] M. Sarikaya, C. Tamerler, A.K.Y. Jen, K. Schulten, F. Baneyx, Nat. Mater. 2 (2003) 577.
[4] S. Brown, Nat. Biotechnol. 15 (1997) 269.
[5] R.R. Naik, S.J. Stringer, G. Agarwal, S.E. Jones, M.O. Stone, Nat. Mater. 1 (2002) 169.
[6] C.K. Thai, H.X. Dai, M.S.R. Sastry, M. Sarikaya, D.T. Schwartz, F. Baneys, Biotechnol. Bioeng. 87 (2004) 129.
[7] D.J.H. Gaskin, K. Starck, E.N. Vulfson, Biotechnol. Lett. 22 (2000) 1211.
[8] S.W. Lee, C.B. Mao, C.E. Flynn, A.M. Belcher, Science 296 (2002) 892.
[9] B.R. Peelle, E.M. Krauland, K.D. Wittrup, A.M. Belcher, Acta Biomater. 1 (2005) 145.

[10] S. Brown, M. Sarikaya, E. Johnson, J. Mol. Biol. 299 (2000) 725.
[11] R. Braun, M. Sarikaya, K.S. Schulten, J. Biomater. Sci. Polym. Ed. 13 (2002) 747.
[12] Y.S. Huh, T.J. Park, E.Z. Lee, W.H. Hong, S.Y. Lee, Electrophoresis 29 (2008) 2960.
[13] T.J. Park, M.S. Hyun, H.J. Lee, S.Y. Lee, S. Ko, Talanta 79 (2009) 295.
[14] T.J. Park, S.Y. Lee, S.J. Lee, J.P. Park, K.S. Yang, K.-B. Lee, S. Ko, J.B. Park, T. Kim, S.K. Kim, Y.B. Shin, B.H. Chung, S.-J. Ku, D.H. Kim, I.S. Choi, Anal. Chem. 78 (2006) 7197.
[15] C. Tamerler, E.E. Oren, M. Duman, E. Venkatasubramanian, M. Sarikaya, Langmuir 22 (2006) 7712.
[16] T.J. Park, S. Zheng, Y.J. Kang, S.Y. Lee, FEMS Microbiol. Lett. 293 (2009) 141.
[17] T.J. Park, J.P. Park, S.J. Lee, H.J. Hong, S.Y. Lee, Biotechnol. Bioproc. Eng. 11 (2006) 173.
[18] T. Endo, K. Kerman, N. Nagatani, H.M. Hiepa, D.-K. Kim, Y. Yonezawa, K. Nakano, E. Tamiya, Anal. Chem. 78 (2006) 6465.
[19] S.Y. Yoo, D.-K. Kim, T.J. Park, E.K. Kim, E. Tamiya, S.Y. Lee, Anal. Chem. 82 (2010) 1349.
[20] A.J. Hase, R.P. Van Duyne, Anal. Bioanal. Chem. 379 (2004) 920.
[21] M. Raghavan, P.J. Bjorkman, Structure 15 (1995) 331.
[22] E. Hutter, J.H. Fendler, Adv. Mater. 16 (2004) 1685.
[23] K.L. Kelly, E. Coronado, L. Zhao, G.C. Schatz, J. Phys. Chem. B 107 (2003) 668.
[24] M.M. Miller, A.A. Lazarides, J. Phys. Chem. B 109 (2005) 21556.
[25] C. Petit, P. Lixon, M.P. Pileni, J. Phys. Chem. 94 (1990) 1598.
[26] L.M. Liz-Marzan, M. Giersig, P. Mulvaney, Langmuir 12 (1996) 4329.
[27] E. Prodan, P. Nordlander, N.J. Halas, Nano Lett. 3 (2003) 1411.